A Dissipative Supramolecular Glue for Temporal Control of Amplified Enzyme Activity and Biocatalytic Cascades

Alisha Kamra,[1] Sourav Das,[1] Preeti Bhatt,[1] Manju Solra,[1] Tanmoy Maity[1] and Subinoy Rana[1,*]

Affiliation:

[1]Materials Research Centre, Indian Institute of Science, C.V. Raman Road, Bangalore 560012, Karnataka, India

***Corresponding Author**

Dr. Subinoy Rana

E-mail: subinoy@iisc.ac.in

Phone : 080-22932914

ABSTRACT

Regulation of enzyme activity is key to the adaptation of cellular processes such as signal transduction and metabolism in response to varying external conditions. Synthetic molecular glues have provided effective systems for enzyme inhibition and regulation of protein-protein interactions. So far, all the molecular glue systems based on covalent interactions operated in equilibrium conditions. To emulate dynamic far-from-equilibrium biological processes, we introduce herein a transient supramolecular glue with controllable lifetime. The transient system uses multivalent supramolecular interactions between guanidium group-bearing surfactants and adenosine triphosphates (ATP), resulting in bilayer vesicle structures. Unlike the conventional fuels for non-equilibrium assemblies, ATP here plays the dual role of providing a structural component for the assembly as well as presenting active functional groups to "glue" enzymes on the surface. While gluing of the enzymes on the vesicles achieves augmented catalysis, oscillation of ATP concentration allows temporal control of the catalytic

activities. We further demonstrate temporal activation and control of biocatalytic cascade networks on the vesicles, which represents an essential cellular component. Altogether, the temporal activation of biocatalytic cascades on the dissipative vesicular glue presents an adaptable and dynamic system emulating heterogeneous cellular processes, opening up avenues for effective protocell construction and therapeutic interventions.

INTRODUCTION

Temporal control of biomolecular components is key to several intracellular reaction networks,[1] robust signal transductions,[2] and efficient cell-cell communications.[3] Likewise, temporal regulation of enzyme activities allows dynamic control of biological transduction[4] and metabolism amongst other processes, helping elucidate biological events at the molecular level[5] and develop therapeutics with low side-effects.[6] While compartmentalized vesicles[7] or scaffold protein-mediated assembly of enzymes[8] allow organization of functional components inside the cell, dynamic regulation of activities requires transient assemblies in response to fuel consumption.[9] Noncovalent interactions enable transient assembly of the active components inside the cell to introduce the dynamic regulatory behavior affecting biomolecular reaction networks,[10-11] assembly of cytoskeletal filaments,[12] cross-talk with organelles,[13-14] and receptor clustering on lipid membranes.[15-16] Further, multiple weak non-covalent interactions such as electrostatics, hydrogen-bonding and van der Waals forces cause adhesion aiding in various biological processes such as the recruitment of white blood cells to inflamed tissue,[17] adherence of influenza virus,[18] and cell division.[19] Synthetic supramolecular systems featuring multivalent non-covalent interactions, termed "molecular glue",[20] provides an efficient scaffold for biomolecular adhesion[21] that have been useful to tailor various natural processes including protein-protein interactions,[22-23] protein-ligand interactions,[24] enzyme inhibition,[25-27] viral inhibition[28-29] and actomyosin sliding motion[21] in a site-selective manner. However, the utility of such molecular glues in the augmentation of the activity of biocatalytic cascades is non-existent. Further, the temporal modulation of the biocatalytic cascades using such molecular glue would provide biomimetic scaffold to designing effective therapeutics and mimic the natural biochemical processes.

Utilizing the principles of systems chemistry, synthetic materials have been introduced to mimic temporal regulation of biocatalytic reactions and biological processes with significant success.[9, 30-31] For example, attempts have been made to drive non-equilibrium assemblies

through catalytic reaction and hydrolytic cleavage of peptides, leading to temporal formation of fibers.[32] Furthermore, the growth and division of protein fibrils in coacervates using guanosine triphosphate,[33] light-responsive self-assembly of micro/nano systems,[34-35] fuel-selective seeded supramolecular polymerization into chiral assembly[36] and ATP-fueled transient nanoreactors to regulate chemical reactions[37] demonstrated dynamic and dissipative processes mimicking cell biology. Various synthetic analogs achieving structural diversities and functions have been introduced including emulsions,[38] hydrogels,[39] nanoreactors,[40] molecular motors,[41] polymersomes[42] and steady-state supramolecular polymers.[43] Use of diverse types of fuels has created a repertoire of complex biomimetic out-of-equilibrium systems such as enzyme-catalyzed pH cycles for the transient control of polymer fluids[44] and breathing microgel,[45] carbodiimide for self-selection of primitive reaction-network,[46] thiols for self-replicating micelles,[47] and DNA for constructing nanodevices for drug release and reaction networks.[31, 48-49] While these fuels provide a structural component for generating the non-equilibrium phases, utilization of the fuels to perform biomolecular functions in the time domain would further enrich our understanding of systems chemistry and produce effective biomimetic scaffolds including molecular adhesives.

In the present study, we introduce a dissipative molecular glue based on a vesicular system (called **VesiGlue**) comprising of a cationic surfactant with guanidium headgroup and ATP as a fuel, which allows effective adhesion for enzymes. Notably, the fuel here serves the dual role of structure and function: (i) to present the essential structural component for the out-of-equilibrium assembly, and (ii) to feature a surface-exposed handle to "glue" the enzymes. Given that CytC binds ATP in an evolutionary conserved pocket[50] without affecting its active site, ATP can act as an allosteric effector of the protein. The adenine moiety is reported to feature physiochemical interactions with proteins through various interactions including electrostatic, H-bonding as well as aromatic and other nonpolar interactions.[51] Moreover, CH/π interaction provides a key driving force for the recognition of DNA and RNA molecules by proteins.[52] We demonstrate here that non-covalent interactions between the latched adenine and enzyme efficiently attaches the enzyme on **VesiGlue** surface, retaining its native tertiary structure. Owing to the increased effective concentration and proximity of the CytC on the vesicle surface, the catalytic activity of the templated enzymes and biocatalytic cascades is upregulated significantly. The amplification of catalytic activity is demonstrated for two more model proteins, validating the generalizability of the **VesiGlue** system. Furthermore, orthogonal catalytic cycles enabling oscillation of the fuel concentration leads to dissociation

of the assembled structures, with concomitant decrease of the enzyme catalysis. However, refueling the **VesiGlue** system enables activation of the biocatalytic cascades in the time domain. The transient activation of individual enzymes and biocatalytic cascades on a biomimetic molecular glue is unprecedented. Furthermore, the temporal regulation of biocatalytic cascades on the vesicular platform effectively mimics the biological processes on heterogenous cellular components. Such transient and autonomous vesicular glues would find important applications in nanomedicines and regenerative medicines by on-demand temporal activation of therapeutic enzymes.

Results and Discussion

ATP-driven self-assembled vesicles

We designed a supramolecular system consisting of a long alkyl chain with varying length (C_n, n = 12, 14, 16, 18) having guanidinium head group that makes a cationic surfactant, which can bind to ATP resulting in ATP-presenting **VesiGlue** surface with the affinity to CytC (Figure 1a). This platform was utilized to modulate the activity of the enzyme. The positively charged guanidinium headgroup was chosen to bind the triphosphate units of ATP through multivalent salt-bridge interactions (Figure 1b)[53] in a wide pH range owing to its high pKa value of 13.6.[54] The C_nGua surfactant were synthesized following the protocol as described in the Supporting Information (SI) Figure S1 and characterized by ^{1}H-NMR, ^{13}C-NMR and mass spectrometry (Figure S2a-c). For the supramolecular system, we explored the ability of C_{16}Gua to form transient assembled structures using ATP as a trivalent capping agent. We utilized ATP to serve three purposes: (i) ATP would provide a multivalent cross-linker, aggregating the surfactants through the favorable guanidium-phosphate salt-bridge interactions, (ii) enzyme-mediated cleavage of the phosphate bond of ATP would lead to energy dissipation, destabilizing the assemblies, and (iii) the adenine group would act as a glue for proteins. The multivalent interaction between ATP and C_nGua was confirmed using ^{31}P NMR. The significant upfield chemical shift values of the α-P from -11.06 to -11.53, β-P from -22.78 to -23.06 and γ-P from -10.7 to -11.08 of ATP (Figure 1c) in the presence of C_{16}Gua shows the molecular recognition between the phosphates of ATP and guanidium units.[55-56] The NMR spectra also demonstrates the stability of phosphates in presence of ligand as the peaks do not diminish.

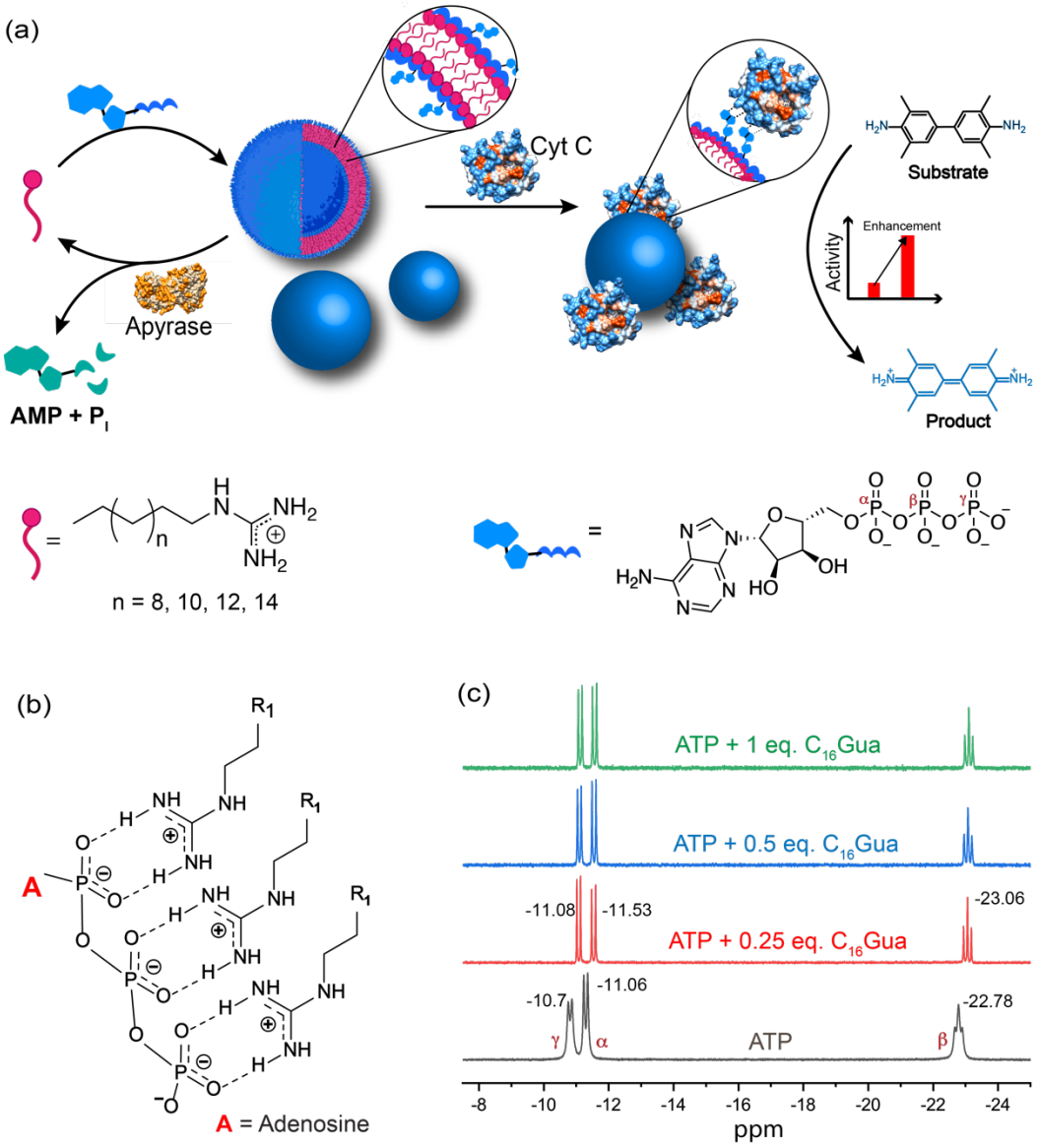

Figure 1. Design of ATP driven self-assembled system. (a) Schematic representation of proposed strategy. (b) Multivalent interactions between the phosphate and guanidium units of the ligand (C_{16}Gua) and (c) ^{31}P NMR Spectra of ATP and C_{16}Gua Complex.

The molecular recognition of C_nGua and ATP leads to discrete aggregates in solution owing to organization of molecules *via* hydrophobic interactions among long alkyl chain and minimized repulsion via charge neutralization of the hydrophilic headgroup. The critical aggregation concentration (CAC) of C_nGua/ATP were determined using 1,6-Diphenyl-1,3,5-hexatriene (DPH) to investigate the change in aggregation behavior in presence of ATP.[57,58] The CAC were found to be approximately 995 µM, 260 µM and 88 µM for C_{14}Gua, C_{16}Gua and C_{18}Gua ligands, respectively (Figure S3a-c). While a concentration below the CAC of the ligand prevents its spontaneous self-assembly, supplying energy through a capping agent (fuel)

may produce a transiently stable out-of-equilibrium system. Addition of ATP to C_{16}Gua resulted in aggregation of the system with 13-fold reduction of CAC to 20 μM (Figure 2a), which is similar to other reported systems on non-equilibrium assemblies.[58-59] A smaller CAC value in presence of ATP indicates the gain in stability of the aggregates.[58, 60] The extent of aggregation is directly dependent on the concentration of ATP (Figure 2b), indicating the presence of intermediate states at sub-saturation concentrations. Moreover, both the fluorescence (Figure 2b) and absorbance (Figure S4) of DPH dye initially increased, which plateaued at an ATP concentration one third that of C_{16}Gua. Therefore, the transiently assembled structures are produced under saturation conditions of 1:3 ATP:C_{16}Gua ratio (henceforth known as **C_{16}VesiGlue**) irrespective of the total concentration of C_{16}Gua (Figure S5), suggesting the assembly formation through the multivalent interactions between triphosphate of one ATP molecule and three molecules of C_{16}Gua ligand. The fluorescence spectra of DPH at 1:3 ATP:C_{16}Gua is shown in Figure S6, where 8-fold enhancement in fluorescence of DPH can be observed upon ATP addition to C_{16}Gua. Accordingly, the average fluorescence lifetime (τ) of DPH showed a substantial increase from 3.934 ns to 5.832 ns upon addition of ATP, which indicates localization of the fluorophore in a structured apolar environment of the **C_{16}VesiGlue** aggregates (Figure 2c).[58] Likewise, the overall surface charge (zeta potential) of the **C_{16}VesiGlue** decreased significantly from the C_{16}Gua ligand alone (Figure S11). The **C_{16}VesiGlue** formed within 10-15 min as demonstrated by the kinetics measurements (Figure S7). Notably, the obtained aggregates were stable for more than 6 h, as revealed by the turbidity measurements (Figure S8). The formation and retention of stability of **C_{16}VesiGlue** in presence of biological concentration[61] of NaCl (150 mM) demonstrates significantly high strength of the salt-bridge interactions between triphosphates and guanidinium (Figure S9).

Next, we investigated the nature of the aggregates and their formation thermodynamics. Initially, we used nanoparticle tracking analysis (NTA) as a robust approach to visualize and track individual colloidal particles in the liquid phase.[62] NTA analysis showed the size distribution of the maximum number of well-defined aggregates to be in the range of 150-250 nm at the 1:3 stoichiometric ratio of ATP:C_{16}Gua (Figure 2d), which is supported by the DLS measurements showing the average hydrodynamic diameter to be ~250 nm (Figure S10). The thermodynamics of **C_{16}VesiGlue** assembly studied by isothermal titration calorimetry (ITC) showed an exothermic binding with a strong affinity of ~10^6 M^{-1}. Furthermore, the molar ratio of ATP to C_{16}Gua was determined to be 1:3 by ITC, supporting the binding stoichiometry

determined by the spectroscopic studies. Besides, the large negative ΔH value indicates the assembly process to be enthalpy driven (Figure 2e). To assess the influence of different fuels with varied valency, we studied the aggregation behavior of C_{16}Gua in presence of adenosine monophosphate (AMP), adenosine diphosphate (ADP), guanosine triphosphate (GTP) and sodium triphosphate (TP). Apparent decrease in the CAC could be observed along with an increase in the turbidity (at 500 nm) of the solution for all the fuels (Figure 2f). Similar to ATP, the triphosphate containing fuels exhibited plateaued turbidity at an XTP/C_{16}Gua (X = G, sodium) stoichiometric ratio of 1:3, whereas diphosphate containing ADP exhibited saturation at a ratio of 1:2. However, the monovalent AMP did not form any assembled structure (Figure 2f), validating the importance of multivalent binding in generating the assembled structures.

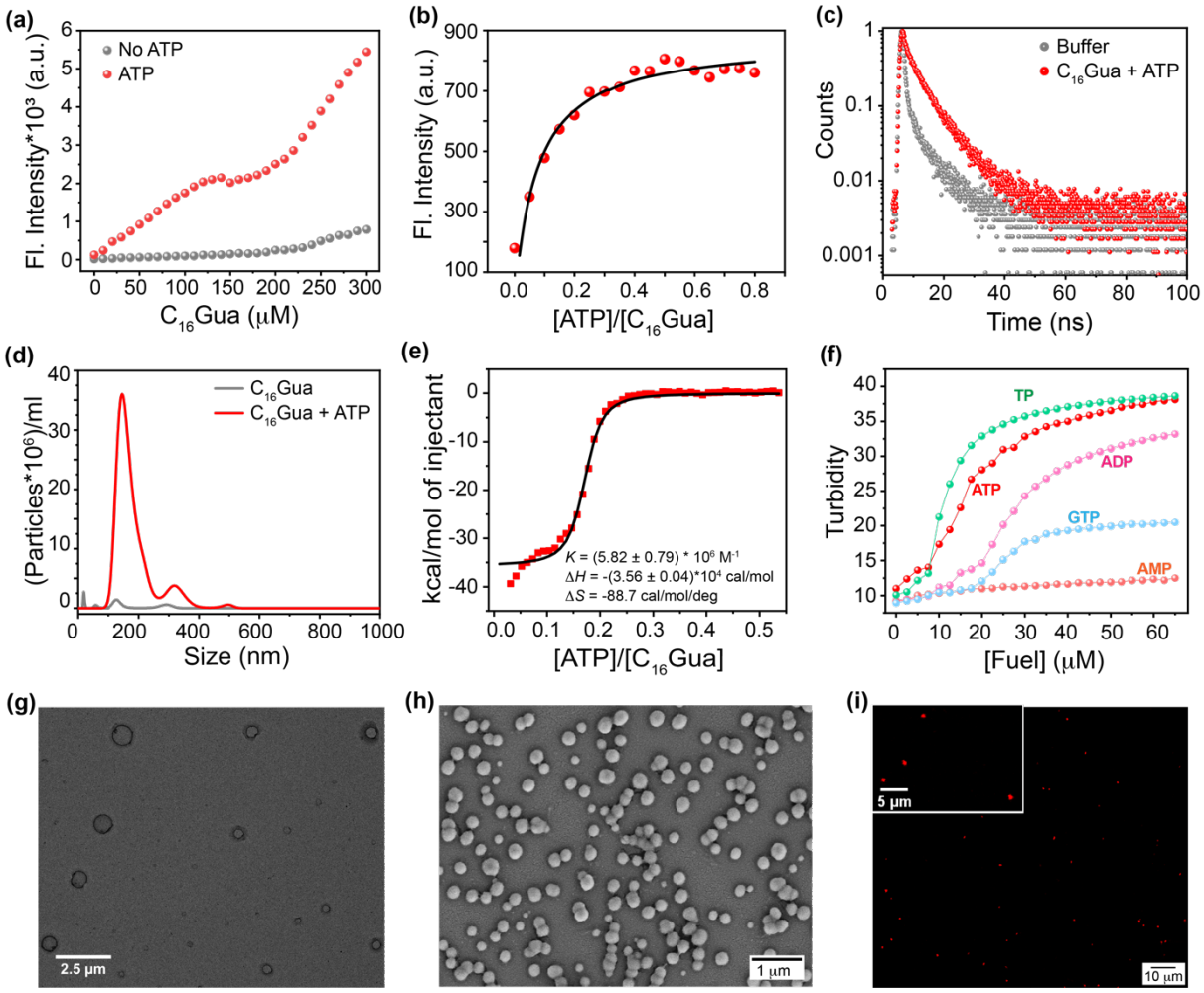

Figure 2. ATP fuel-dependent assembly. (a) Fluorescence intensity of DPH Dye at 428 nm with increasing concentration of C_{16}Gua in presence and absence of ATP (33 μM). (b) Fluorescence intensity at 428 nm as a function of the concentration of ATP added to an aqueous buffered solution containing 100 μM of C_{16}Gua and DPH as the fluorescent hydrophobic probe. (c) Time-domain intensity decay of

DPH in aqueous buffer, excited by a 375 nm laser. (d) Nanoparticle Tracking Analysis of the **C_{16}VesiGlue** assembly in buffer. (e) ITC data of ATP binding to C_{16}Gua. ITC data was obtained for titration of ATP into 100 µM C_{16}Gua. (f) Turbidity measurement by titrating 100 µM C_{16}Gua with increasing concentration of ATP, TP, GTP, ADP and AMP in buffer. (g) TEM image of **C_{16}VesiGlue**. (h) SEM image of **C_{16}VesiGlue**. (i) Confocal image of Nile red entrapped **C_{16}VesiGlue**.

To further elucidate the size and morphology of the **C_{16}VesiGlue** aggregates, various analytical techniques were utilized. Transmission electron microscopy (TEM) and field emission scanning electron microscopy (FESEM) images demonstrate that the aggregates present a vesicular morphology with diameters 150-250 nm (Figure 2g and 2h, respectively). Notably, the TEM images showed a higher contrast at the boundary of the spherical assemblies that indicates the presence of bilayer structures.[63] However, the C_{16}Gua alone at the same concentration did not produce any assembly (Figure S12). To visually observe the distribution of a hydrophobic fluorophore (Nile red) in the assembled structures, the sample was 3D scanned by confocal laser scanning microscopy (CLSM) (Figure 2i). Although the size of the assemblies falls below the resolving power of CLSM, the accumulation of nile red dye in the apolar bilayer of the **C_{16}VesiGlue** allowed the structures to be detected. It can be observed that the dye gets entrapped within the hydrophobic domain of the spherical vesicles (Figure 2i). All these results support the formation of self-assembled bilayer vesicles *via* noncovalent salt-bridge interactions between guanidinium and triphosphate.

VesiGlue for molecular recognition of proteins

Modulation of the enzymatic activity of proteins by synthetic materials is an important aspect in protein-based bioengineering as well as to understand the diverse range of reactions inside the cells and predict the metabolism of living things.[64] Therefore, we investigated the possibility of temporally regulating the activity of an enzyme using the self-assembled **C_{16}VesiGlue**. Given the importance of CytC enzyme in the electron transport chain,[65] we studied the peroxidase activity of CytC templated on the vesicle surfaces. First, CLSM imaging was performed using Nile red-entrapped **C_{16}VesiGlue** and FITC-tagged CytC to determine if CytC is "glued" to **C_{16}VesiGlue** surface. As illustrated in Figure 3a, the green fluorescence of FITC-labelled CytC is decorated on the **C_{16}VesiGlue** surface, whereas distinguishable fluorescent structures were never observed in absence of ATP. The gluing of CytC was further probed by the native fluorescence of ATP that decreases upon interaction with another

molecule.[66] The ATP fluorescence at 360 nm decreased 1.4-folds upon addition of C_{16}Gua to ATP at the CAC. The fluorescence emission of ATP further decreased with the addition of CytC (Figure 3b), indicating favorable biochemical interaction between CytC and ATP present on the **C_{16}VesiGlue** surface. Furthermore, the increased average particles size (Figure 3c) from 180 nm to 300 nm observed in NTA upon addition of CytC further suggests its templation on the surface of **C_{16}VesiGlue**. Formation of the protein corona over the **VesiGlue** surface results in the crowding of few vesicles *via* aggregation resulting in increased size, similar to what is observed for liposomal platforms.[67] The result was further supported by DLS measurements (Figure S13), wherein the hydrodynamic diameter was found to be ~450 nm. To study the stability of ATP-fueled **C_{16}VesiGlue** upon CytC anchoring, DPH dye leakage assay was performed. No significant change in the fluorescence of DPH upon CytC addition suggests that the dye is not replaced by the protein and hence the **C_{16}VesiGlue** remain intact when CytC is anchored on its surface (Figure 3d). Moreover, no replacement of dye from the **C_{16}VesiGlue** suggests that CytC is bound to surface rather than going into the hydrophobic domain.

The specific molecular recognition of CytC by **C_{16}VesiGlue** has been proven via ITC measurements as well as later by the activity assays. ITC study showed that the CytC interacts with **C_{16}VesiGlue** with a binding affinity of 2.99×10^5 M^{-1} (Figure 3e), which is ~3-fold stronger than the affinity of CytC with TP-templated aggregates (1.18×10^5 M^{-1}) (Figure S14a). This demonstrates the importance of adenine unit of ATP for the specific non-covalent binding with the amino acids of CytC *via* supramolecular interactions.[51] The most important factors contributing to the negative values of enthalpy and entropy, and hence to the stability of protein glued on **C_{16}VesiGlue**, are van der Waals interactions.[68] Further, the binding affinity of CytC with GTP-assisted aggregates was much less (3.7×10^4 M^{-1}) compared to that of ATP (Figure S14b). The result proves the specific binding of adenine's donor and acceptor atoms with the protein mainly via electrostatics and H-bonding interactions.[51]

The impact on the native structure of the protein upon binding with **C_{16}VesiGlue** was monitored using UV−vis spectroscopy that can detect any change in the micro-environment near the heme center. In addition to the peak at 280 nm, CytC has three characteristic peaks centered at 360 (δ band), 409 (Soret band), and 530 nm (Q band).[69] These bands remain unaffected upon attachment to **C_{16}VesiGlue** (Figure 3f), suggesting that the active site of CytC remains intact. The integrity of the protein structure was further assessed by circular dichroism (CD) that showed no significant deviation or alteration of the ellipticity corresponding to the characteristic peaks at 208 and 222 nm of the protein (Figure 3g). Therefore, the secondary

structure of CytC remained unchanged in the presence of the self-assembled **C_{16}VesiGlue**. While the reported micellar systems with exposed charged groups[70] and amphiphilic homopolymer[71] showed alteration of CytC structure, the **C_{16}VesiGlue** system provides a non-denaturing platform that retains the protein structure. The intact secondary structure of the protein also indicates that CytC latches onto the surface of the assembly rather than being embedded within the hydrophobic domain.[70, 72] Taken together, all these results coupled with (a) the favorable interaction between the neutral **C_{16}VesiGlue** and cationic protein, and (b) the negative controls of GTP, AMP, triphosphate at their corresponding CACs, point at the nature of gluing interaction being multivalent non-covalent interaction between the exposed ATP on **C_{16}VesiGlue** surface and CytC.

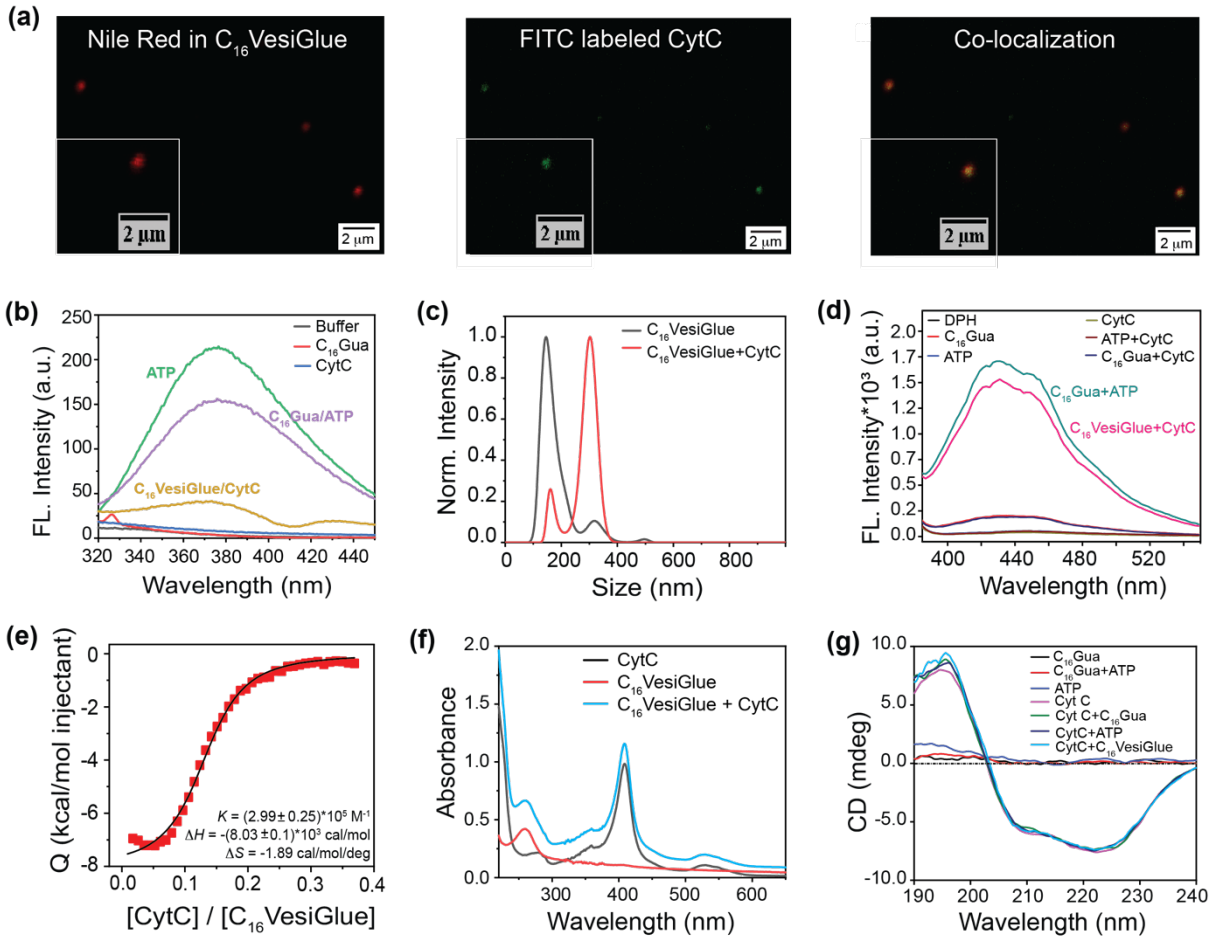

Figure 3. Vesicular glue for the molecular recognition of proteins. (a) Co-localization of FITC-labeled CytC (green) on assembly (red) visualized by Confocal Microscopy. (b) Fluorescence intensity of ATP (Ex. 260 nm). (c) NTA measurement in buffer for **C_{16}VesiGlue** (50 μM C_{16}Gua and 33 μM ATP) in presence of CytC (0.5 μM). (d) Zeta potential measurement of XTP/C_{16}Gua (X = G, sodium) system (33 μM/100 μM) in presence of CytC (0.5 μM), performed in buffer. (e) Fluorescence intensity of DPH (Ex.

355 nm). ITC data was obtained for titration of CytC into **C_{16}VesiGlue** solution (f) in buffer and (g) in presence of 100 mM salt concentration. (h) UV-Vis spectra of CytC (black), **VesiGlue** (red) and CytC in presence of **VesiGlue** (blue). (i) CD Spectra of CytC in buffer and CytC in presence of **VesiGlue** with other controls.

Augmented enzyme activity on VesiGlue

Given the retention of CytC native structure, we investigated whether the enzymatic activity of the enzyme is modulated on the **C_{16}VesiGlue** surface. The peroxidase activity of CytC was studied by monitoring the rate of conversion of the substrate 3,3′,5,5′-tetramethylbenzidine (TMB) to 3,3′,5,5′-tetramethylbenzidine diamine (TMB_{ox}) in the presence of oxidant H_2O_2.[73] As observed from Figure 4a, ATP alone increases the specific activity of CytC by 3.2 fold, which got further enhanced by 8.4 fold when CytC is bound to ATP on the vesicle surface. The augmented activity arises from the increased local concentration of CytC and proximity, when attached onto the vesicle surface.[74] Interestingly, the same equivalents of TP-assisted assembly did not exhibit any enhancement of the CytC peroxidase activity (Figure 4a), clearly demonstrating the essence of adenine group of ATP that interacts with CytC *via* non-covalent interactions including electrostatic, H-bonding, and aromatic interactions.[51] Notably, GTP-fueled assemblies failed to enhance the enzyme activity (Figure 4a), which supports the importance of adenine in the molecular recognition of the enzyme on the **C_{16}VesiGlue** surface. Although, the assembly containing hydrophobic compartment is formed in case of C_{16}Gua with different fuels (TP and GTP) as well, the lack of CytC activity enhancement in these assemblies clearly demonstrates the importance of ATP as a recognition site for CytC. Besides, the activity of CytC@**C_{16}VesiGlue** is enhanced linearly with the increasing concentration of the **C_{16}VesiGlue** (Figure 4b), validating the templation effect of the vesicular glue. The catalytic activity of CytC increases as a function of reaction time (Figure S15). To understand the kinetic behavior of the system, the catalytic activity of CytC@**C_{16}VesiGlue** was measured at different concentrations of H_2O_2 (Figure 4c). The kinetic pattern suggests that the CytC glued on **C_{16}VesiGlue** follows the Michaelis-Menten model. The kinetic parameters were determined by Lineweaver-Burk plot (Figure 4d) and are shown in SI Table 1. The K_M (Michaelis constant) value of 42.6 μM for native CytC was significantly reduced to 20.9 μM when bound to **C_{16}VesiGlue**, suggesting the substantially enhanced substrate affinity of the enzyme glued on **C_{16}VesiGlue**. The high k_{cat} of CytC@**C_{16}VesiGlue** indicates much higher catalytic efficiency compared to the unbound CytC.

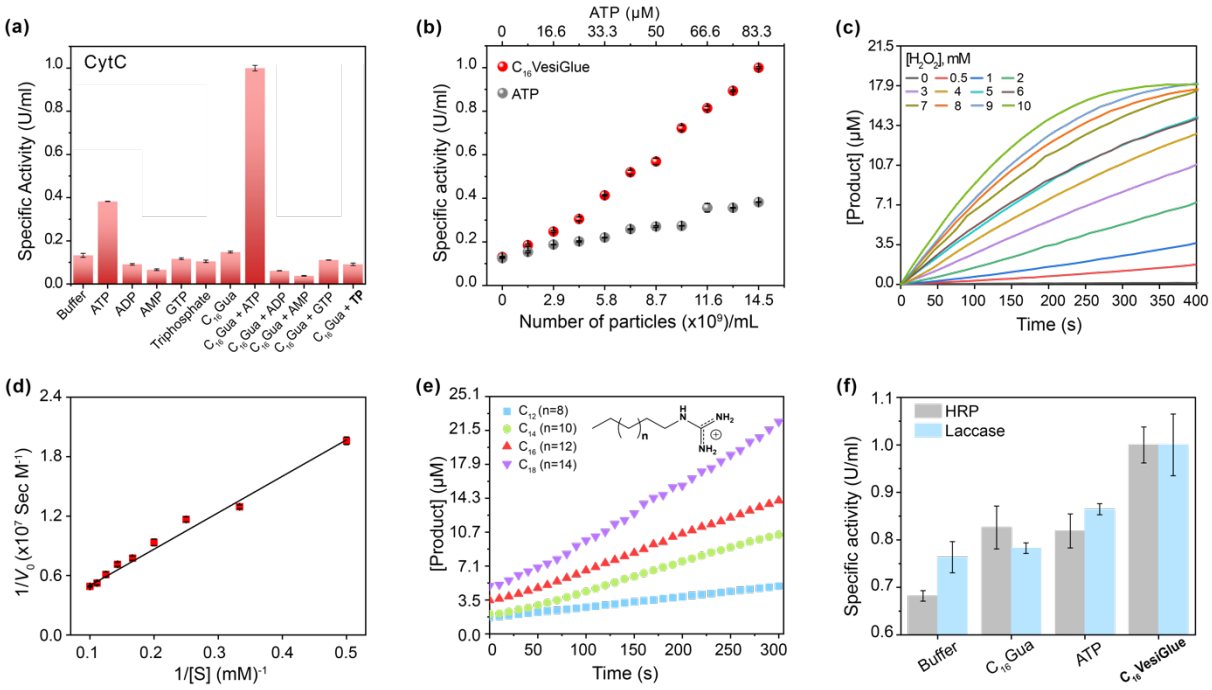

Figure 4. Augmented enzyme activity on vesicular glue. (a) Relative specific activity of CytC in presence of assembly formed via different fuels. (b) Specific activity of CytC in presence of varying **C_{16}VesiGlue** concentration (particles per mL measured by NTA) vs only ATPs. (c) Increase in absorbance at 650 nm upon TMB oxidation in presence of CytC anchored on **C_{16}VesiGlue** with time. (d) Lineweaver-Burk plot of CytC activity anchored on **VesiGlue**. (e) Specific activity of CytC anchored on **VesiGlues** with varying chain length of ligand. (f) Specific activity of HRP and Laccase in presence of **C_{16}VesiGlue**. All the specific activities have been normalized to the maximum value.

Further, we studied the effect of alkyl chain length of the guanidium-terminated ligands in modulating the activity of CytC. For **VesiGlues** of varied alkyl chain lengths of C_{12}, C_{14}, C_{16}, and C_{18}, an increased activity was observed (Figure 4e). Consequently, a 6-fold difference in specific activity was observed between the C_{12} and C_{18} ligands, which could be due to the significant size difference between the assemblies formed by the two (Figure S10b). We further examined the difference in stability of vesicles formed by **C_{16}Gua**/ATP and cetyltrimethylammonium chloride (CTAC)/ATP and their ability to upregulate the enzymatic activity. It was found that the CytC activity enhancement by CTAC/ATP structures was about 2.5-fold less than the **C_{16}VesiGlue** (Figure S16). Therefore, the salt bridge interaction between guanidium and phosphates of **C_{16}VesiGlue** provides stronger non-covalent bonding than the simple electrostatic interaction between quaternary ammonium group and phosphates in the CTAC/ATP vesicles. Next, the specific activities of horseradish peroxidase (HRP) and laccase enzymes were measured to examine the versatility of the template effect of the system (Figure

4f). Activity of HRP was monitored by the extent of oxidation of TMB as a substrate.[75] The specific activity of HRP was enhanced by 1.5 folds in presence of **C_{16}VesiGlue**. ABTS was used as a substrate to study the oxidase like activity of laccase decorated on the **C_{16}VesiGlue**.[76] It was observed that laccase activity enhanced by 1.3-fold in presence of **C_{16}VesiGlue**, which further proves the versatility of the system. Altogether, vesicular glue provides a robust and generalized platform to augment the catalytic activity of different enzymes.

Cascade reactions on the VesiGlue surface

A cascade reaction is a multistep chemical reaction in which a substrate is transformed into a product that becomes a substrate for the subsequent reaction.[77] Biomolecular cascades play central role in multiple biological processes including cell response towards a stimulus, initiation of blood coagulation, production of carbohydrates through photosynthesis, etc.[78] We demonstrate a two-step cascade reaction using glucose oxidase (GOx) and **C_{16}VesiGlue** templated CytC. GOx is an oxidoreductase enzyme that catalyzes the aerobic oxidation of glucose to gluconic acid with the simultaneous formation of H_2O_2, fueling the second catalytic reaction of TMB in presence of CytC (Figure 5a). For the two-step cascade reaction, the activity was monitored by adding the substrate glucose along with TMB as the chromogenic substrate for the terminal cascade reaction, producing a greenish blue product (Figure 5a). The catalytic activity of the cascade reaction was enhanced as the concentration of GOx enzyme was increased, monitored by absorbance of oxidized TMB at 650 nm (Figure 5b, c). Moreover, the kinetics of oxidized TMB product formation was monitored by UV/Vis spectroscopy (λ_{em}= 652 nm, Figure 5d) showing the increased product formation with time. The activity of the cascade by GOx/CytC/**C_{16}VesiGlue** was found to be 0.223 ± 0.0014 μM min^{-1} with 0.3 nM of GOx and 5 mM of glucose, plotted as relative specific activity of CytC (Figure 5e). Interestingly, cascade activity in the presence of **C_{16}VesiGlue** was 6.5-fold higher compared to the controls of free GOx/CytC diffusional mixture at the same concentration. However, separately used CytC/**C_{16}VesiGlue** and GOx/**C_{16}VesiGlue** did not show any noticeable activity (Figure 5e), indicating the crucial role of the **VesiGlue** templated cascade reaction in producing the oxidized product. Moreover, the GOx/CytC/**C_{16}VesiGlue** cascade reaction showed a linear dependence on the substrate (glucose) concentration (Figure 5f). Besides, the linear standard curve showed detectable signal even at a concentration of 10 μM (3×standard deviation of the blank), demonstrating high sensitivity of the platform toward glucose. Overall, these results

suggest that "gluing" the enzymes on the vesicle surface helps facilitating the cascade reaction *via* increasing the local effective concentration of the substrates.[74]

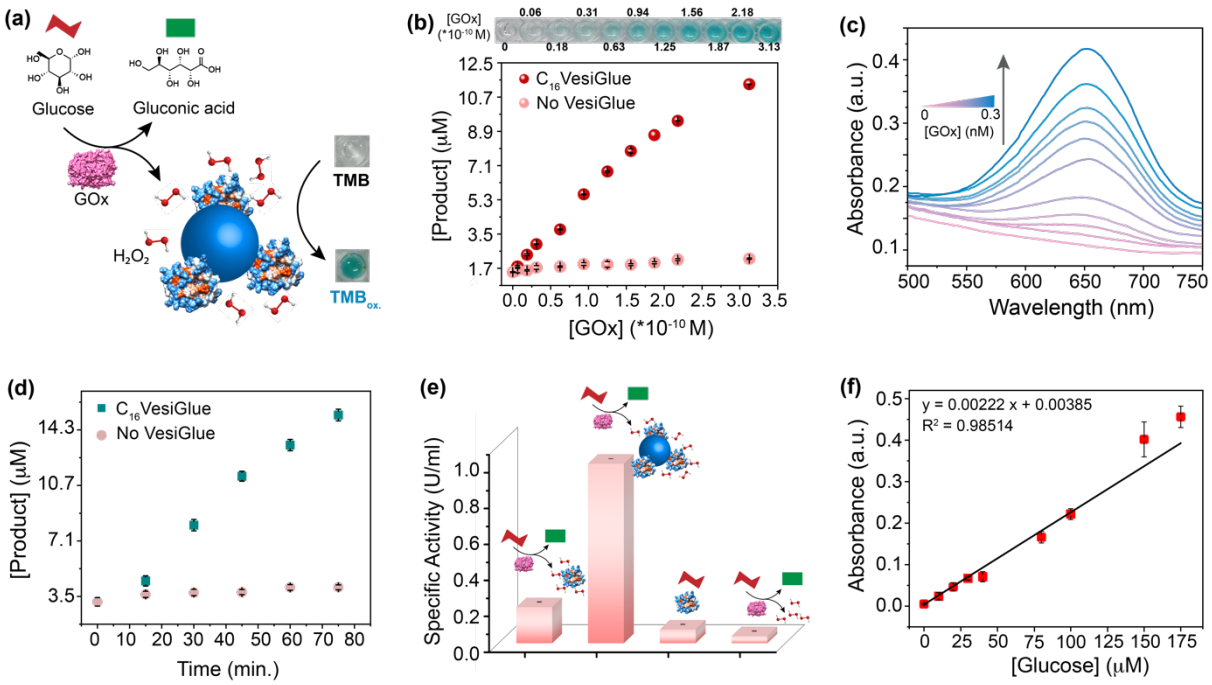

Figure 5. Cascade reaction on the **VesiGlue** surface. (a) Schematics for cascade reaction on **VesiGlue** surface. (b) Absorbance of oxidized TMB (TMB_{ox}) at λ_{em} 650 nm with varying concentration of GOx (0 - 0.3 nM), color of oxidized TMB in inset. (c) The absorbance spectra of TMB_{ox} with increasing GOx concentration. (d) Absorbance of TMB_{ox} at 650 nm as a function of time in presence and absence of **VesiGlue**. (e) Specific activity of CytC under different conditions of cascading. (f) The GOx/CytC/**C_{16}VesiGlue** cascade reaction with increasing glucose concentration.

Temporal control of enzyme activity and biocatalytic cascade

We tested the efficacy of **VesiGlue** to regulate the augmented enzyme activity in the time domain as long as the fuel is present, emulating biological processes such as signal transduction, transport, and cell division.[1, 79] Given the ATP-dependent **VesiGlue** formation, we hypothesized that oscillation of ATP concentration could switch between two distinct, transient states in a recyclable, out-of-equilibrium process. To achieve the goal, another cycle requires to be introduced that utilizes the ATP as a fuel followed by its conversion to inactive waste with concomitant destabilization of the system.[80] We achieved this cycle using potato apyrase (PA) enzyme, which hydrolyses ATP to adenosine 5′-monophosphate (AMP) and two molecules of orthophosphate (P_i).[81] The produced AMP and P_i with a monovalent phosphate

unit does not stabilize the assembly (Figure 2f), resulting in the disassembly of C_{16}Gua surfactants. In the absence of PA, the fluorescence signal of DPH remained constant in time upon ATP addition to C_{16}Gua, indicating the stability of the **VesiGlue** under these conditions. However, the presence of different PA concentrations (0-1 U/mL) led to a decay in fluorescence signal depending on the PA concentration (Figure 6a) due to the breakdown of the **C_{16}VesiGlue**. 1 U/mL of apyrase could break almost 90% assembly formed by 50 μM C_{16}Gua and 16.6 μM ATP in ~40 min. We studied the oscillatory behavior through fluorescence intensity-time trajectory using DPH dye sequestration in the assembled structures. Consequent refueling the system with 0.5 eq. of ATP leads to gradual enhancement of the DPH emission intensity to ~100% of the initial intensity before breakage, suggesting the reformation of the **C_{16}VesiGlue** (Figure 6b). Requirement of higher equivalents of ATP to reach 100% of initial fluorescence values on subsequent additions signifies the competing effect of the biproducts (AMP + Pi).[40] The lack of multivalent interactions of ATP in presence of PA could not induce the vesicle formation as observed from the decreased particles (from 5.8×10^9/mL to 7.1×10^8/mL) and non-uniform size distribution through NTA study (Figure 6c). The instability of the assembly could also be visualized by confocal microscopy *via* addition of PA to Nile red entrapped **C_{16}VesiGlue**,[82] resulting in decreased particles in sometime (Figure 6d). The results demonstrate the transient formation of vesicle in presence of ATP as a fuel.

Next, the temporal regulation of enzyme activity on the **VesiGlue** surfaces was attempted to mimic the adaptive biological systems with temporal control of enzyme activities upon consumption of energy. Specifically, we investigated the activity of the templated enzyme as long as the system stays in the out-of-equilibrium state in the form of the **VesiGlue**. Regulation of enzymatic activity in the time domain was studied using CytC glued onto the C_{16}Gua/ATP system, and PA to utilize the fuel that transforms the system to equilibrium. Given the interference of PA on TMB oxidation, the activity of CytC was measured using a well-known substrate pyrogallol. The substrate upon the catalyzed-oxidation in presence of H_2O_2 converts to purpurogallin and shows a yellow color with λ_{max} = 420 nm.[72] The augmented specific activity of CytC attached to the **VesiGlue** was gradual downregulated as the PA slowly disintegrated the **C_{16}VesiGlue**, which was dependent on the **VesiGlue** and PA concentrations (Figure 6e). Each subsequent addition of 0.5 equivalents of ATP led to upregulation of the peroxidase-like activity of CytC to the initial specific activity. Autonomous oscillation was demonstrated for three complete cycles without losing considerable enzyme activity (Figure 6f), indicating continuous operation as long as the fuel is present. The time dependent CytC

activity regulation for the three consecutive cycles is shown in Figure 6g. Therefore, we demonstrated successful modulation of CytC activity on the ATP templated **VesiGlue**. This temporal regulation of enzyme activity underscores the subtle but significant role of the transiently assembled vesicular glue.

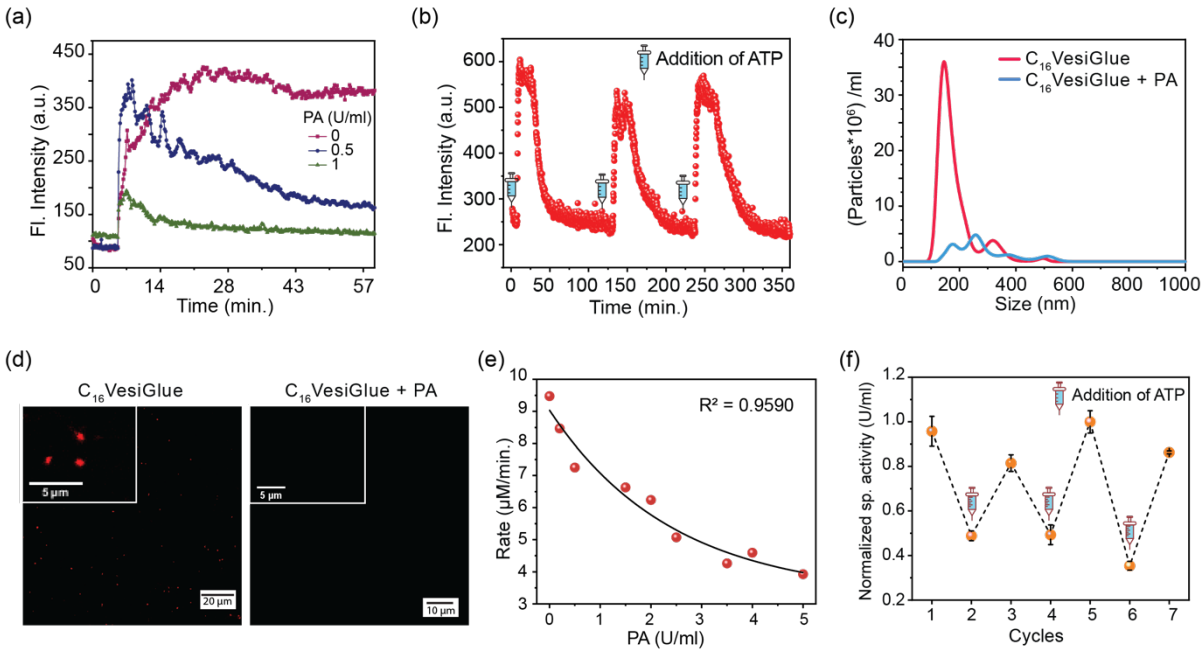

Figure 6. Temporal control of enzyme activity. (a) Fluorescent intensity at 428 nm as a function of time following addition of ATP to C_{16}Gua and DPH in the presence of different concentrations of potato apyrase. (b) Fluorescence intensity following three repetitive additions of ATP to a solution of C_{16}Gua and DPH in the presence of potato apyrase. (c) NTA measurement of **VesiGlue** in presence and absence of apyrase, where the area under the graph represents total number of particles/mL. (d) Confocal images of fluorophore trapped assembly in absence and presence of PA. (e) Rate of purpurogallin formation with increasing PA concentration on **VesiGlue**. (f) Temporal regulation of specific activity of CytC-catalyzed oxidation of pyrogallol with repetitive addition of ATP to the solution containing **VesiGlue** and PA.

CONCLUSIONS

In summary, we have successfully demonstrated the generation of an ATP-fueled out-of-equilibrium vesicular glue that can upregulate activities of diverse enzymes. Compared to the previously reported traditional non-equilibrium systems utilizing the fuel as a structural component, we show, for the first time, that the fuel can perform an active function of attaching proteins on the vesicle surface using multivalent non-covalent interactions. The efficacy of the

system was further realized in the activation of biocatalytic cascades with augmented enzymatic reactions. Moreover, the **VesiGlue** show dissipative behavior in presence of apyrase enzyme that consumes the fuel ATP. Based on the observation, we successfully constructed a transient vesicular glue that is fueled by ATP in presence of apyrase, with a tunable lifetime. Consequently, temporal regulation of individual enzymes and catalytic cascades is achieved in response to the fuel oscillation. These results present an entirely new way of temporally modulating biocatalytic cascades using a supramolecular vesicular glue, emulating the natural systems. Therefore, we believe that the present generalized approach will allow the development of new life-like systems with time-gated enzyme activity regulation on cellular components including extracellular vesicles.

Beyond the utility of the out-of-equilibrium **VesiGlue** as a model system mimicking the transient biological processes, the concept can be extended to expedited chemical synthesis, and biomedical applications. For example, directed evolution of proteins against the adenine group or other substituted phosphates would provide specific molecular regulation of therapeutic proteins,[83] with regulated activity in the time domain. Likewise, the transient enzymatic cascades with upregulated activity can potentially have therapeutic applications,[49] such as the temporal control of intracellular signaling agents[84] or the dose-dependent generation of reactive oxygen species as therapeutics.[85] Furthermore, the current study on dissipative vesicles with protein corona show great promise in providing delivery vehicle for permeation in cellular organelle and intervene with the cellular processes.

ASSOCIATED CONTENT

Supporting Information: The Supporting Information is available. Synthesis and characterization data of the C_nGua and fuel dependent assembly's spectroscopic data, additional experimental data of UV-Vis, fluorescence, SEM and ITC, Supporting Figures S1 – S27 and Table S1.

AUTHOR INFORMATION

Corresponding Author

Subinoy Rana - Materials Research Centre, Indian Institute of Science, Bangalore 560012, Karnataka, India

Email: subinoy@iisc.ac.in

Authors

Alisha Kamra - Materials Research Centre, Indian Institute of Science, Bangalore 560012, Karnataka, India

Email: alishakamra@iisc.ac.in

Sourav Das - Materials Research Centre, Indian Institute of Science, Bangalore 560012, Karnataka, India

Email: souravd@iisc.ac.in

Preeti Bhatt - Materials Research Centre, Indian Institute of Science, Bangalore 560012, Karnataka, India

Email: preetibhatt@iisc.ac.in

Manju Solra - Materials Research Centre, Indian Institute of Science, Bangalore 560012, Karnataka, India

Email: manjusolra@iisc.ac.in

Tanmoy Maity - Materials Research Centre, Indian Institute of Science, Bangalore 560012, Karnataka, India

Email: tanmoymaity@alum.iisc.ac.in

Notes

The authors declare no competing financial interest.

ACKNOWLEDGEMENTS

S.R. acknowledges major financial support from MoE-STARS (STARS/APR2019/BS/820/FS). The Science and Engineering Research Board (ECR/2018/00255) is acknowledged for financial support to accessing the IISc central facilities. Seed funding by the IISc Digital Health Initiative is acknowledged for some consumables. The authors are thankful to the Department of Science and Technology (DST-FIST: SR/FST/PSII009/2010) for the instrumental facility at MRC. A.K. and P.B. are thankful to Prime Minister Research Fellowship for doctoral research. M.S. and T.M. are thankful to UGC and MoE, respectively, for the doctoral research

fellowships. Financial support from the DBT-RA Program in Biotechnology and Life Sciences is gratefully acknowledged by S.D.

REFERENCES

1. Mofatteh, M.; Echegaray-Iturra, F.; Alamban, A.; Dalla Ricca, F.; Bakshi, A.; Aydogan, M. G., Autonomous clocks that regulate organelle biogenesis, cytoskeletal organization, and intracellular dynamics. *eLife* **2021,** *10*, e72104.
2. Bhattacharyya, R. P.; Reményi, A.; Yeh, B. J.; Lim, W. A., Domains, motifs, and scaffolds: the role of modular interactions in the evolution and wiring of cell signaling circuits. *Annual review of biochemistry* **2006,** *75* (1), 655-680.
3. Kholodenko, B. N.; Hancock, J. F.; Kolch, W., Signalling ballet in space and time. *Nature reviews Molecular cell biology* **2010,** *11* (6), 414-426.
4. Wijnands, S. P. W.; Engelen, W.; Lafleur, R. P. M.; Meijer, E. W.; Merkx, M., Controlling protein activity by dynamic recruitment on a supramolecular polymer platform. *Nat. Commun.* **2018,** *9* (1), 65.
5. Seo, H.; Lee, H., Spatiotemporal control of signal-driven enzymatic reaction in artificial cell-like polymersomes. *Nat. Commun.* **2022,** *13* (1), 5179.
6. Zhu, S.; Nih, L.; Carmichael, S. T.; Lu, Y.; Segura, T., Enzyme-Responsive Delivery of Multiple Proteins with Spatiotemporal Control. *Adv. Mater.* **2015,** *27* (24), 3620-3625.
7. Chen, A. H.; Silver, P. A., Designing biological compartmentalization. *Trends in cell biology* **2012,** *22* (12), 662-670.
8. Good, M. C.; Zalatan, J. G.; Lim, W. A., Scaffold proteins: hubs for controlling the flow of cellular information. *Science* **2011,** *332* (6030), 680-686.
9. Boekhoven, J.; Hendriksen, W. E.; Koper, G. J.; Eelkema, R.; van Esch, J. H., Transient assembly of active materials fueled by a chemical reaction. *Science* **2015,** *349* (6252), 1075-1079.
10. Ngo, T. A.; Nakata, E.; Saimura, M.; Morii, T., Spatially Organized Enzymes Drive Cofactor-Coupled Cascade Reactions. *J. Am. Chem. Soc.* **2016,** *138* (9), 3012-3021.
11. Xin, L.; Zhou, C.; Yang, Z.; Liu, D., Regulation of an Enzyme Cascade Reaction by a DNA Machine. *Small* **2013,** *9* (18), 3088-3091.
12. Fletcher, D. A.; Mullins, R. D., Cell mechanics and the cytoskeleton. *Nature* **2010,** *463* (7280), 485-492.
13. Banani, S. F.; Lee, H. O.; Hyman, A. A.; Rosen, M. K., Biomolecular condensates: organizers of cellular biochemistry. *Nat. Rev. Mol. Cell Biol.* **2017,** *18* (5), 285-298.
14. Shin, Y.; Brangwynne, C. P., Liquid phase condensation in cell physiology and disease. *Science* **2017,** *357* (6357), eaaf4382.
15. Casaletto, J. B.; McClatchey, A. I., Spatial regulation of receptor tyrosine kinases in development and cancer. *Nat. Rev. Cancer* **2012,** *12* (6), 387-400.
16. Hartman, N. C.; Groves, J. T., Signaling clusters in the cell membrane. *Curr. Opin. Cell Biol.* **2011,** *23* (4), 370-376.
17. Albelda, S. M.; Buck, C. A., Integrins and other cell adhesion molecules. *The FASEB journal* **1990,** *4* (11), 2868-2880.
18. Mammen, M.; Choi, S. K.; Whitesides, G. M., Polyvalent interactions in biological systems: implications for design and use of multivalent ligands and inhibitors. *Angewandte Chemie International Edition* **1998,** *37* (20), 2754-2794.

19. Nasmyth, K.; Haering, C. H., Cohesin: its roles and mechanisms. *Annual review of genetics* **2009,** *43*, 525-558.
20. Schreiber, S. L., The Rise of Molecular Glues. *Cell* **2021,** *184* (1), 3-9.
21. Okuro, K.; Kinbara, K.; Takeda, K.; Inoue, Y.; Ishijima, A.; Aida, T., Adhesion Effects of a Guanidinium Ion Appended Dendritic "Molecular Glue" on the ATP-Driven Sliding Motion of Actomyosin. *Angew. Chem., Int. Ed.* **2010,** *49* (17), 3030-3033.
22. Li, F.; Aljahdali, I. A. M.; Ling, X., Molecular Glues: Capable Protein-Binding Small Molecules That Can Change Protein-Protein Interactions and Interactomes for the Potential Treatment of Human Cancer and Neurodegenerative Diseases. *Int. J. Mol. Sci.* **2022,** *23* (11).
23. Mogaki, R.; Okuro, K.; Ueki, R.; Sando, S.; Aida, T., Molecular Glue that Spatiotemporally Turns on Protein–Protein Interactions. *J. Am. Chem. Soc.* **2019,** *141* (20), 8035-8040.
24. Mogaki, R.; Okuro, K.; Aida, T., Molecular glues for manipulating enzymes: trypsin inhibition by benzamidine-conjugated molecular glues. *Chemical Science* **2015,** *6* (5), 2802-2805.
25. Okuro, K.; Sasaki, M.; Aida, T., Boronic Acid-Appended Molecular Glues for ATP-Responsive Activity Modulation of Enzymes. *J. Am. Chem. Soc.* **2016,** *138* (17), 5527-5530.
26. Ju, E.; Wang, F.; Wang, Z.; Liu, C.; Dong, K.; Pu, F.; Ren, J.; Qu, X., Modular AND Gate-Controlled Delivery Platform for Tumor Microenvironment Specific Activation of Protein Activity. *Chem.Eur.J* **2020,** *26* (34), 7573-7577.
27. St-Cyr, D.; Ceccarelli, D. F.; Orlicky, S.; van der Sloot, A. M.; Tang, X.; Kelso, S.; Moore, S.; James, C.; Posternak, G.; Coulombe-Huntington, J.; Bertomeu, T.; Marinier, A.; Sicheri, F.; Tyers, M., Identification and optimization of molecular glue compounds that inhibit a noncovalent E2 enzyme-ubiquitin complex. *Sci. Adv.* **2021,** *7* (44), eabi5797.
28. Nie, C.; Stadtmüller, M.; Yang, H.; Xia, Y.; Wolff, T.; Cheng, C.; Haag, R., Spiky Nanostructures with Geometry-matching Topography for Virus Inhibition. *Nano Lett.* **2020,** *20* (7), 5367-5375.
29. Vonnemann, J.; Sieben, C.; Wolff, C.; Ludwig, K.; Böttcher, C.; Herrmann, A.; Haag, R., Virus inhibition induced by polyvalent nanoparticles of different sizes. *Nanoscale* **2014,** *6* (4), 2353-2360.
30. Estirado, E. M.; Rosier, B. J.; de Greef, T. F.; Brunsveld, L., Dynamic modulation of proximity-induced enzyme activity using supramolecular polymers. *Chemical Communications* **2020,** *56* (43), 5747-5750.
31. Ouyang, Y.; Zhang, P.; Willner, I., Dissipative biocatalytic cascades and gated transient biocatalytic cascades driven by nucleic acid networks. *Science Advances* **2022,** *8* (18), eabn3534.
32. Debnath, S.; Roy, S.; Ulijn, R. V., Peptide Nanofibers with Dynamic Instability through Nonequilibrium Biocatalytic Assembly. *J. Am. Chem. Soc.* **2013,** *135* (45), 16789-16792.
33. Te Brinke, E.; Groen, J.; Herrmann, A.; Heus, H. A.; Rivas, G.; Spruijt, E.; Huck, W. T., Dissipative adaptation in driven self-assembly leading to self-dividing fibrils. *Nat. Nanotechnol.* **2018,** *13* (9), 849-855.
34. Zhao, H.; Sen, S.; Udayabhaskararao, T.; Sawczyk, M.; Kučanda, K.; Manna, D.; Kundu, P. K.; Lee, J.-W.; Král, P.; Klajn, R., Reversible trapping and reaction acceleration within dynamically self-assembling nanoflasks. *Nat. Nanotechnol.* **2016,** *11* (1), 82-88.
35. Kundu, P. K.; Samanta, D.; Leizrowice, R.; Margulis, B.; Zhao, H.; Börner, M.; Udayabhaskararao, T.; Manna, D.; Klajn, R., Light-controlled self-assembly of non-photoresponsive nanoparticles. *Nat. Chem.* **2015,** *7* (8), 646-652.
36. Mishra, A.; Korlepara, D. B.; Kumar, M.; Jain, A.; Jonnalagadda, N.; Bejagam, K. K.; Balasubramanian, S.; George, S. J., Biomimetic temporal self-assembly via fuel-driven controlled supramolecular polymerization. *Nat. Commun.* **2018,** *9* (1), 1-9.
37. Cardona, M. A.; Prins, L. J., ATP-fuelled self-assembly to regulate chemical reactivity in the time domain. *Chem. Sci.* **2020,** *11* (6), 1518-1522.
38. Schwarz, P. S.; Tebcharani, L.; Heger, J. E.; Müller-Buschbaum, P.; Boekhoven, J., Chemically fueled materials with a self-immolative mechanism: transient materials with a fast on/off response. *Chem. Sci.* **2021,** *12* (29), 9969-9976.

39. Heuser, T.; Weyandt, E.; Walther, A., Biocatalytic Feedback-Driven Temporal Programming of Self-Regulating Peptide Hydrogels. *Angewandte Chemie International Edition* **2015,** *54* (45), 13258-13262.
40. Maiti, S.; Fortunati, I.; Ferrante, C.; Scrimin, P.; Prins, L. J., Dissipative self-assembly of vesicular nanoreactors. *Nature Chemistry* **2016,** *8* (7), 725-731.
41. Wilson, M. R.; Solà, J.; Carlone, A.; Goldup, S. M.; Lebrasseur, N.; Leigh, D. A., An autonomous chemically fuelled small-molecule motor. *Nature* **2016,** *534* (7606), 235-240.
42. Rikken, R.; Engelkamp, H.; Nolte, R.; Maan, J.; Van Hest, J.; Wilson, D.; Christianen, P., Shaping polymersomes into predictable morphologies via out-of-equilibrium self-assembly. *Nat. Commun.* **2016,** *7* (1), 1-7.
43. Sorrenti, A.; Leira-Iglesias, J.; Sato, A.; Hermans, T. M., Non-equilibrium steady states in supramolecular polymerization. *Nat. Commun.* **2017,** *8* (1), 1-8.
44. Hao, X.; Yang, K.; Wang, H.; Peng, F.; Yang, H., Biocatalytic feedback-controlled non-Newtonian fluids. *Angew. Chem., Int. Ed.* **2020,** *59* (11), 4314-4319.
45. Che, H.; Buddingh', B. C.; van Hest, J. C., Self-Regulated and Temporal Control of a "Breathing" Microgel Mediated by Enzymatic Reaction. *Angew. Chem.* **2017,** *129* (41), 12755-12759.
46. Schnitter, F.; Bergmann, A. M.; Winkeljann, B.; Rodon Fores, J.; Lieleg, O.; Boekhoven, J., Synthesis and characterization of chemically fueled supramolecular materials driven by carbodiimide-based fuels. *Nat. Protoc.* **2021,** *16* (8), 3901-3932.
47. Howlett, M. G.; Engwerda, A. H. J.; Scanes, R. J. H.; Fletcher, S. P., An autonomously oscillating supramolecular self-replicator. *Nature Chemistry* **2022,** *14* (7), 805-810.
48. Del Grosso, E.; Ragazzon, G.; Prins, L. J.; Ricci, F., Fuel-responsive allosteric DNA-based aptamers for the transient release of ATP and cocaine. *Angewandte Chemie* **2019,** *131* (17), 5638-5642.
49. Wang, J.; Li, Z.; Willner, I., Cascaded dissipative DNAzyme-driven layered networks guide transient replication of coded-strands as gene models. *Nat. Commun.* **2022,** *13* (1), 4414.
50. Craig, D. B.; Wallace, C. J., ATP binding to cytochrome c diminishes electron flow in the mitochondrial respiratory pathway. *Protein science : a publication of the Protein Society* **1993,** *2* (6), 966-76.
51. Narunsky, A.; Kessel, A.; Solan, R.; Alva, V.; Kolodny, R.; Ben-Tal, N., On the evolution of protein-adenine binding. *Proceedings of the National Academy of Sciences of the United States of America* **2020,** *117* (9), 4701-4709.
52. Chakrabarti, P.; Samanta, U., CH/pi interaction in the packing of the adenine ring in protein structures. *Journal of molecular biology* **1995,** *251* (1), 9-14.
53. Onda, M.; Yoshihara, K.; Koyano, H.; Ariga, K.; Kunitake, T., Molecular Recognition of Nucleotides by the Guanidinium Unit at the Surface of Aqueous Micelles and Bilayers. A Comparison of Microscopic and Macroscopic Interfaces. *Journal of the American Chemical Society* **1996,** *118* (36), 8524-8530.
54. Caine, B. A.; Bronzato, M.; Fraser, T.; Kidley, N.; Dardonville, C.; Popelier, P. L. A., Aqueous pKa prediction for tautomerizable compounds using equilibrium bond lengths. *Communications Chemistry* **2020,** *3* (1), 21.
55. Khatua, S.; Choi, S. H.; Lee, J.; Kim, K.; Do, Y.; Churchill, D. G., Aqueous fluorometric and colorimetric sensing of phosphate ions by a fluorescent dinuclear zinc complex. *Inorg Chem* **2009,** *48* (7), 2993-9.
56. Dey, S.; Sarkar, T.; Majumdar, A.; Pathak, T.; Ghosh, K., 1,4-Disubstituted 1,2,3-Triazole- and 1,5-Disubstituted 1,2,3-Triazole–based Bis-Sulfonamides in Selective Fluorescence Sensing of ATP. *ChemistrySelect* **2017,** *2* (6), 2034-2038.
57. Cui, X.; Mao, S.; Liu, M.; Yuan, H.; Du, Y., Mechanism of Surfactant Micelle Formation. *Langmuir* **2008,** *24* (19), 10771-10775.
58. Maiti, S.; Fortunati, I.; Ferrante, C.; Scrimin, P.; Prins, L. J., Dissipative self-assembly of vesicular nanoreactors. *Nat Chem* **2016,** *8* (7), 725-31.

59. Sasaki, R.; Murata, S., Aggregation of Amphiphilic Pyranines in Water: Facile Micelle Formation in the Presence of Methylviologen. *Langmuir* **2008,** *24* (6), 2387-2394.
60. Cardona, M. A.; Prins, L. J., ATP-fuelled self-assembly to regulate chemical reactivity in the time domain. *Chemical Science* **2020,** *11* (6), 1518-1522.
61. Strazzullo, P.; Leclercq, C., Sodium. *Advances in nutrition (Bethesda, Md.)* **2014,** *5* (2), 188-90.
62. Comfort, N.; Cai, K.; Bloomquist, T. R.; Strait, M. D.; Ferrante, A. W., Jr.; Baccarelli, A. A., Nanoparticle Tracking Analysis for the Quantification and Size Determination of Extracellular Vesicles. *Journal of visualized experiments : JoVE* **2021,** (169), 10.3791/62447.
63. Silvander, M.; Karlsson, G.; Edwards, K., Vesicle Solubilization by Alkyl Sulfate Surfactants: A Cryo-TEM Study of the Vesicle to Micelle Transition. *J. Colloid Interface Sci.* **1996,** *179* (1), 104-113.
64. Schena, A.; Griss, R.; Johnsson, K., Modulating protein activity using tethered ligands with mutually exclusive binding sites. *Nature Communications* **2015,** *6* (1), 7830.
65. Hüttemann, M.; Pecina, P.; Rainbolt, M.; Sanderson, T. H.; Kagan, V. E.; Samavati, L.; Doan, J. W.; Lee, I., The multiple functions of cytochrome c and their regulation in life and death decisions of the mammalian cell: From respiration to apoptosis. *Mitochondrion* **2011,** *11* (3), 369-81.
66. Amat, A.; Rigau, J.; Waynant, R. W.; Ilev, I. K.; Tomas, J.; Anders, J. J., Modification of the intrinsic fluorescence and the biochemical behavior of ATP after irradiation with visible and near-infrared laser light. *J. Photochem. Photobiol., B* **2005,** *81* (1), 26-32.
67. Corbo, C.; Molinaro, R.; Taraballi, F.; Toledano Furman, N. E.; Sherman, M. B.; Parodi, A.; Salvatore, F.; Tasciotti, E., Effects of the protein corona on liposome-liposome and liposome-cell interactions. *International journal of nanomedicine* **2016,** *11*, 3049-63.
68. Ross, P. D.; Subramanian, S., Thermodynamics of protein association reactions: forces contributing to stability. *Biochemistry* **1981,** *20* (11), 3096-3102.
69. Wu, L.; Jiang, X., Enhancing Peroxidase Activity of Cytochrome c by Modulating Interfacial Interaction Forces with Graphene Oxide. *Langmuir* **2020,** *36* (5), 1094-1102.
70. Rani, S.; Dasgupta, B.; Bhati, G. K.; Tomar, K.; Rakshit, S.; Maiti, S., Superior Proton-Transfer Catalytic Promiscuity of Cytochrome c in Self-Organized Media. *ChemBioChem* **2021,** *22* (7), 1285-1291.
71. Sandanaraj, B. S.; Bayraktar, H.; Krishnamoorthy, K.; Knapp, M. J.; Thayumanavan, S., Recognition and Modulation of Cytochrome c's Redox Properties using an Amphiphilic Homopolymer. *Langmuir* **2007,** *23* (7), 3891-3897.
72. Saha, B.; Chatterjee, A.; Reja, A.; Das, D., Condensates of short peptides and ATP for the temporal regulation of cytochrome c activity. *Chemical Communications* **2019,** *55* (94), 14194-14197.
73. Wen, J.; He, D.; Yu, Z.; Zhou, S., In situ detection of microbial c-type cytochrome based on intrinsic peroxidase-like activity using screen-printed carbon electrode. *Biosens. Bioelectron.* **2018,** *113*, 52-57.
74. Carver, A. M.; De, M.; Bayraktar, H.; Rana, S.; Rotello, V. M.; Knapp, M. J., Intermolecular electron-transfer catalyzed on nanoparticle surfaces. *J Am Chem Soc* **2009,** *131* (11), 3798-9.
75. Volpe, G.; Draisci, R.; Palleschi, G.; Compagnone, D., 3,3′,5,5′-Tetramethylbenzidine as electrochemical substrate for horseradish peroxidase based enzyme immunoassays. A comparative study. *Analyst* **1998,** *123* (6), 1303-1307.
76. Reiss, R.; Ihssen, J.; Richter, M.; Eichhorn, E.; Schilling, B.; Thöny-Meyer, L., Laccase versus laccase-like multi-copper oxidase: a comparative study of similar enzymes with diverse substrate spectra. *PLoS One* **2013,** *8* (6), e65633.
77. Chatterjee, A.; Mahato, C.; Das, D., Complex Cascade Reaction Networks via Cross β Amyloid Nanotubes. *Angew. Chem., Int. Ed.* **2021,** *60* (1), 202-207.
78. Li, L.; Chen, K.; Wu, Y.; Xiang, G.; Liu, X., Epigenome-Metabolome-Epigenome signaling cascade in cell biological processes. *J. Genet. Genomics* **2021**.
79. Moraru, I. I.; Loew, L. M., Intracellular signaling: spatial and temporal control. *Physiology* **2005,** *20* (3), 169-179.

80. van Rossum, S. A. P.; Tena-Solsona, M.; van Esch, J. H.; Eelkema, R.; Boekhoven, J., Dissipative out-of-equilibrium assembly of man-made supramolecular materials. *Chemical Society Reviews* **2017,** *46* (18), 5519-5535.
81. Lomakina, G. Y.; Konik, P. A.; Ugarova, N. N., The Kinetics of Hydrolysis of ATP by Apyrase A from Solanum tuberosum. *Moscow University Chemistry Bulletin* **2020,** *75* (6), 374-381.
82. Iwai, M.; Ikeda, K.; Shimojima, M.; Ohta, H., Enhancement of extraplastidic oil synthesis in Chlamydomonas reinhardtii using a type-2 diacylglycerol acyltransferase with a phosphorus starvation–inducible promoter. *Plant biotechnology journal* **2014,** *12*.
83. Miller, D. C.; Athavale, S. V.; Arnold, F. H., Combining chemistry and protein engineering for new-to-nature biocatalysis. *Nature Synthesis* **2022,** *1* (1), 18-23.
84. Assadi, S. M.; Yücel, M.; Pantelis, C., Dopamine modulates neural networks involved in effort-based decision-making. *Neurosci. Biobehav. Rev.* **2009,** *33* (3), 383-93.
85. Kang, R. H.; Kim, Y.; Kim, J. H.; Kim, N. H.; Ko, H. M.; Lee, S.-H.; Shim, I.; Kim, J. S.; Jang, H.-J.; Kim, D., Self-Activating Therapeutic Nanoparticle: A Targeted Tumor Therapy Using Reactive Oxygen Species Self-Generation and Switch-on Drug Release. *ACS Appl. Mater. Interfaces* **2021,** *13* (26), 30359-30372.